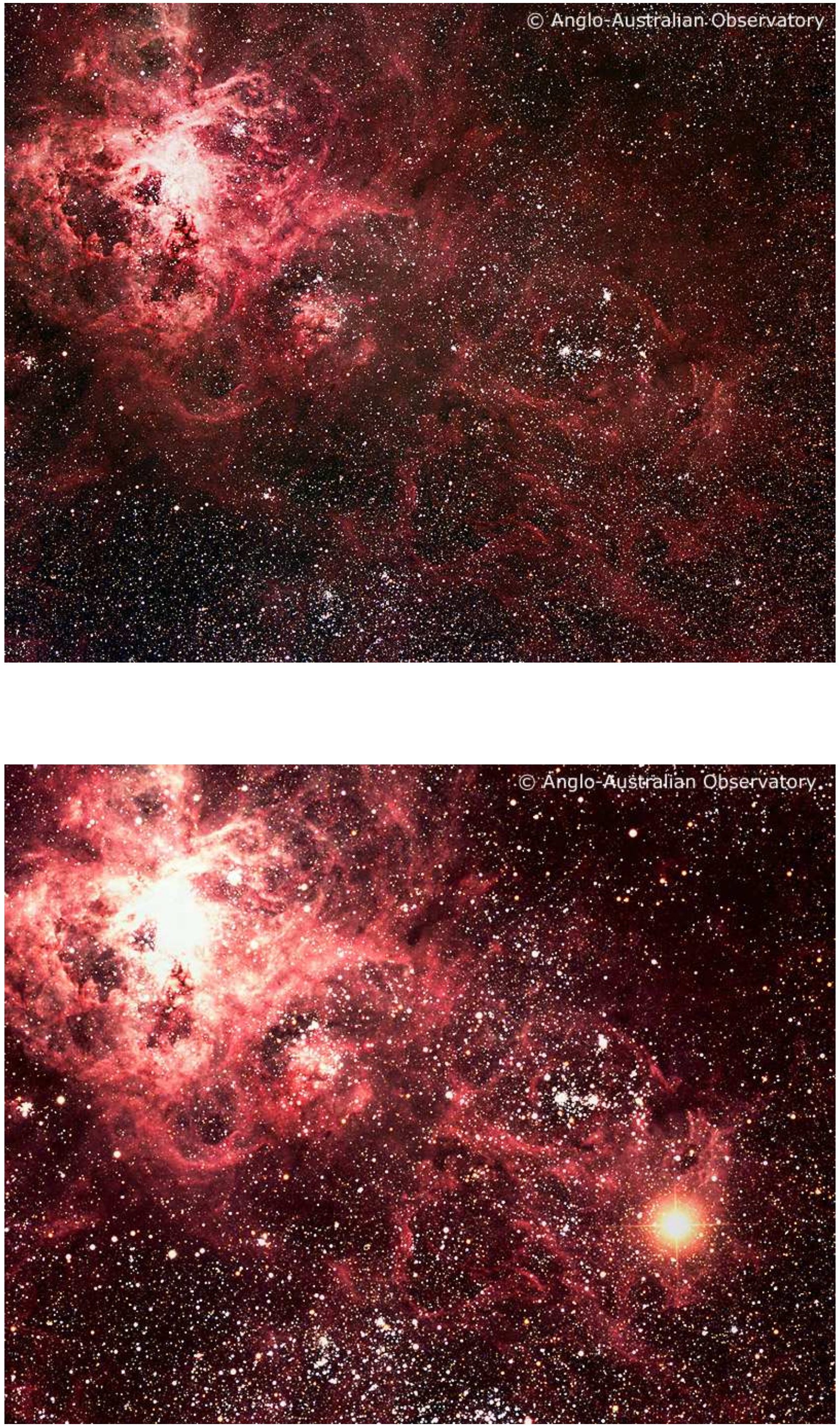

1987 February: Supernova in Large Magellanic Cloud.

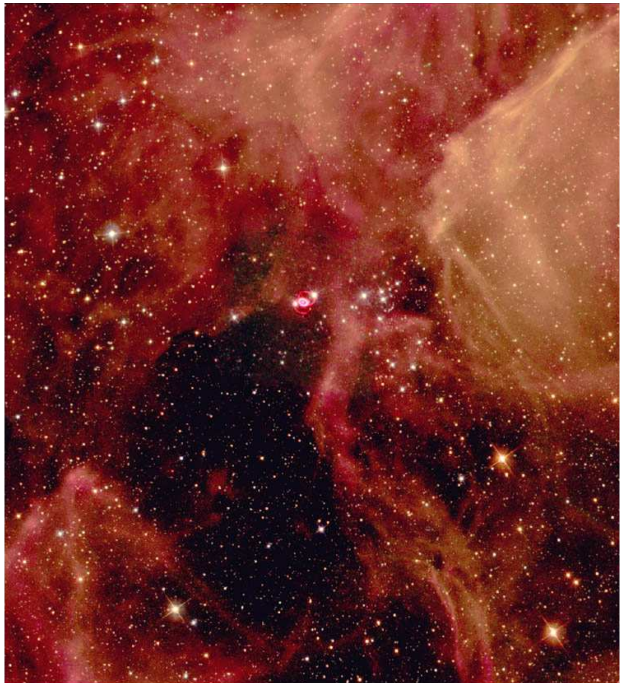

HST/NASA/ESA/STScI

STScI PR94-22

87 d after explosion: Ring ($1.66'' \times 1.21''$) of ionized C and N around SN

$\Longrightarrow$ Excitation of C, N in ring-like shell (ejecta from red giant phase of progenitor?): “light echo”

LMC: Distance

Light echo: direct geometrical determination of distance to LMC possible:

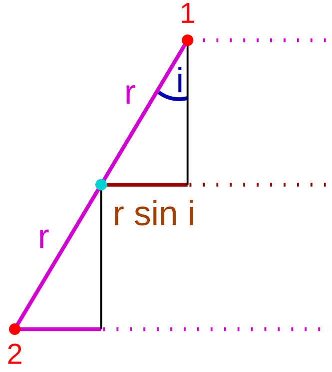

Time delay SN: close side of ring:

$$ct_1 = r(1 - \sin i) = 86 \pm 6\,\text{d} \tag{3.1}$$

Time delay SN: far side of ring:

$$ct_2 = r(1 + \sin i) = 413 \pm 24\,\text{d} \tag{3.2}$$

The ring radius is:

$$r = c\,\frac{t_1 + t_2}{2} = 250 \pm 12\,\text{ltd} \tag{3.3}$$

and the inclination is:

$$\sin i = \frac{t_2 - t_1}{t_1 + t_2} \quad \Longrightarrow \quad i \sim 41^\circ \tag{3.4}$$

(From ring-geometry: $\cos i = 1''\!.21/1''\!.66 \Longrightarrow i \sim 43^\circ$)

Thus from angular size of ring:

$$1''\!.66 = \frac{r \cos i}{d} \quad \Longrightarrow \quad d = 52 \pm 3\,\text{kpc} \tag{3.5}$$

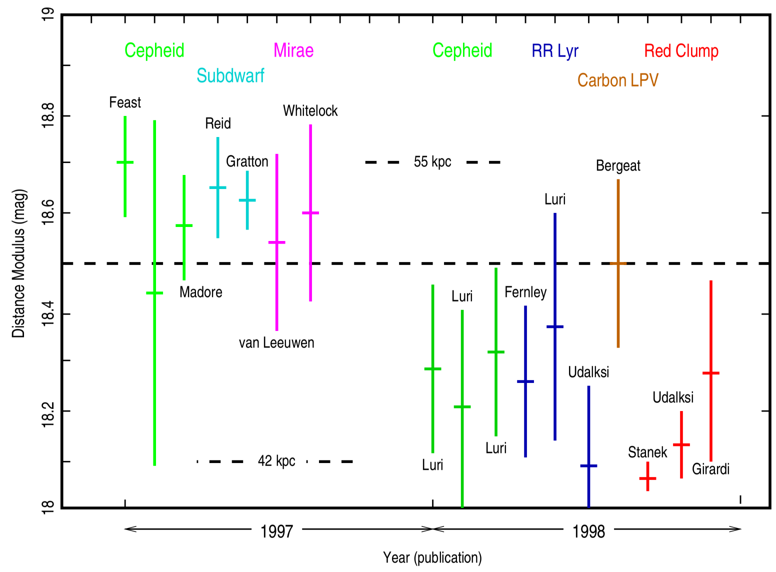

LMC distance: "anchor point" of extragalactic distance scale.

After Gaia Science Workgroup

Strong dependence on Hipparcos calibration.

DM ranges between 18.7 ± 0.1 mag (Feast & Catchpole) and 18.57 ± 0.11 mag (Madore & Freedman)

Currently, the distance to the LMC is less well known than desirable.

LMC: Metallicity

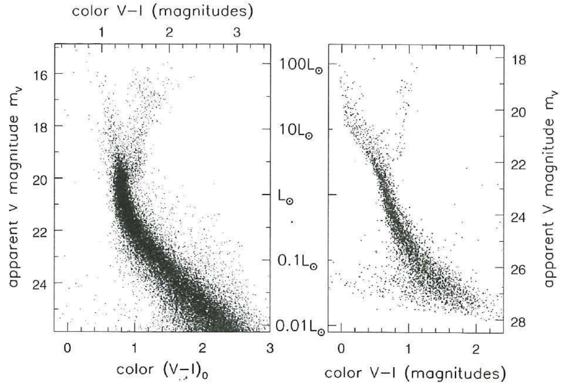

Sparke & Gallagher, Fig. 4.5

CMD of bulge stars in the MW | CMD of stars in LMC

Wide main sequence ⟹ dispersion in stellar ages

LMC: MS is bluer ⟹ LMC has lower metallicity

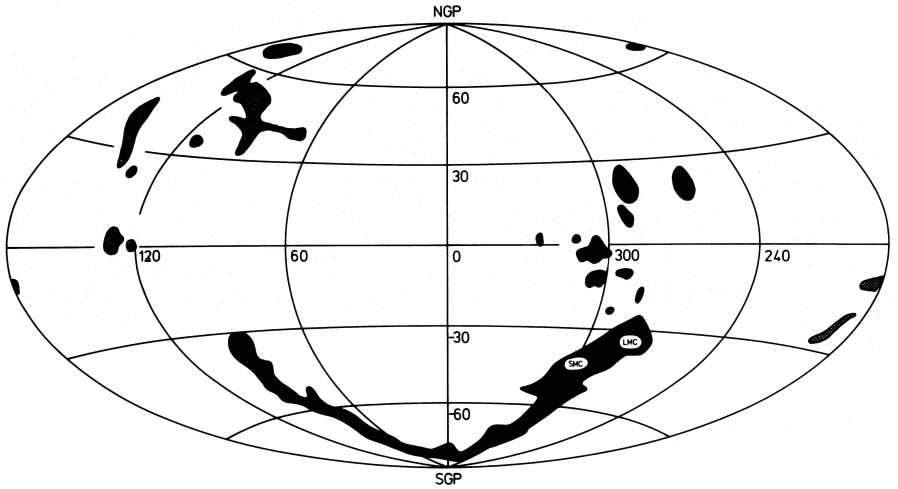

Mathewson et al. (1974, Fig. 1):

Magellanic Stream: number of high velocity clouds trailing Magellanic clouds

Total mass: $2 \times 10^8\,M_\odot$.

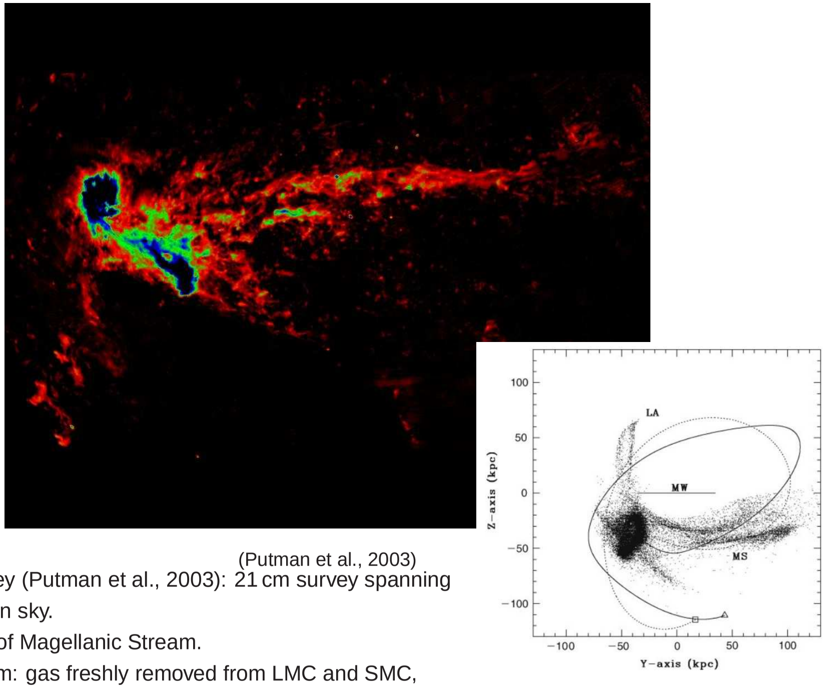

(Putman et al., 2003)

HIPASS-Survey (Putman et al., 2003): 21 cm survey spanning whole southern sky.

first real map of Magellanic Stream.

Head of stream: gas freshly removed from LMC and SMC, tail: older material

(Bekki & Chiba, 2009, Fig. 3)

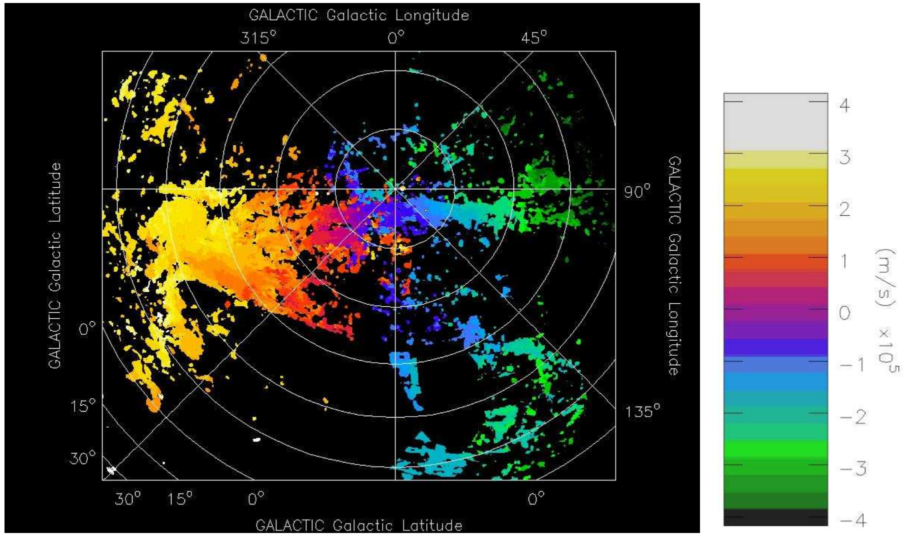

(Putman et al., 2003)

Velocity field from HIPASS-Survey

Stream has gradient of ∼700 km s^{-1}, ∼390 km s^{-1} faster than galactic rotation

⟹ noncircular orbit

R. Gendler

General Properties

Andromeda galaxy:

- diameter 20 kpc, distance 675 kpc
- ∼50% more luminous than Galaxy
- faster rotation speed (∼260 km/s)
- 300 globular clusters
- many satellites:
  - one elliptical galaxy (M32)
  - three dwarf ellipticals
  - at least six dwarf spheroidals

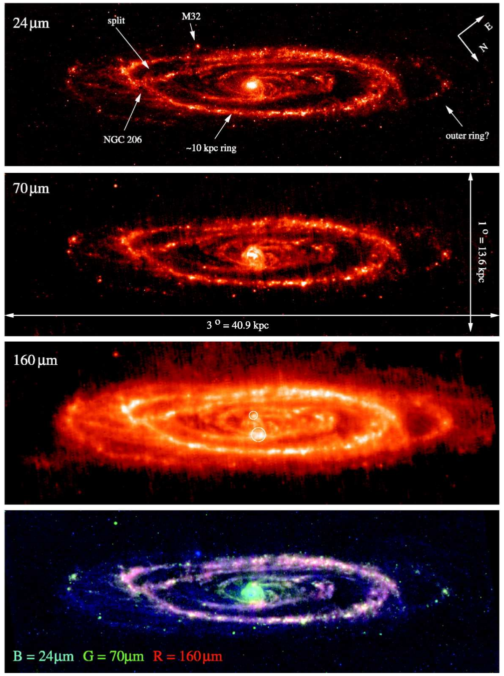

Dust distribution in M31:

- “ring of fire” at $\sim$10 kpc
- contains most young stars
- also contains ionized H II regions (see last lecture)

(Gordon et al., 2006, Fig. 1)

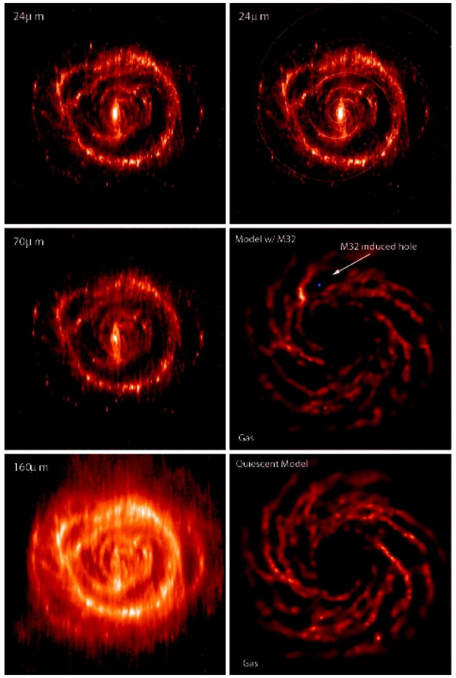

Deprojected images of Andromeda assuming inclination of 75°

Note clear spiral structure, but disturbed by passage of M32 (first seen by ISO.

Movie time: `gordon_video1.mpg`

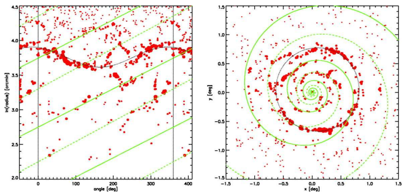

Ring is off-center, not associated directly with spiral arms (modeled by logarithmic spiral); origin not completely clear.

(Gordon et al., 2006, Figs. 3 and 4)

Dust

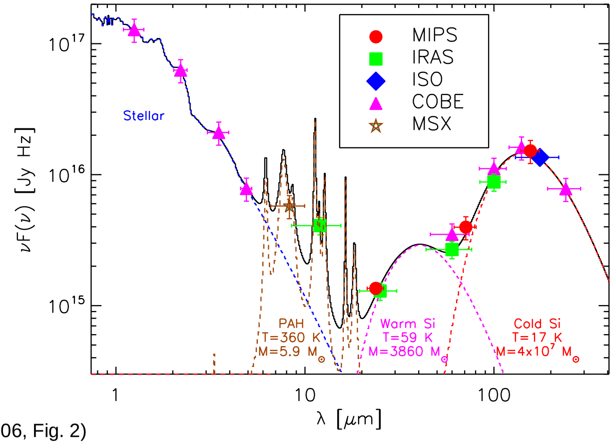

(Gordon et al., 2006, Fig. 2)

Total IR luminosity: 1.7×10^{43} erg s^{-1}, corresponding to star formation rate of 0.75 $M_\odot$ yr^{-1}.

Dust composition: silicates (warm from inner regions, cold from outer regions of Galaxy) and some polycyclic aromatic hydrocarbons (PAHs)

Milky Way and M31

M31 and Milky Way are gravitationally bound and approaching on a collision course, with collision happening in 2 billion years.

Possible scenario: formation of an elliptical galaxy over the course of about 1 billion years.

Collision studied with numerical simulations, movies show evolution calculations using 307.2 million particles (10 days on 512 processors):

MOVIE Time: `hdmwa.mov` and `7_FutureSky.avi` from `http://www.cita.utoronto.ca/~dubinski/nbody/`

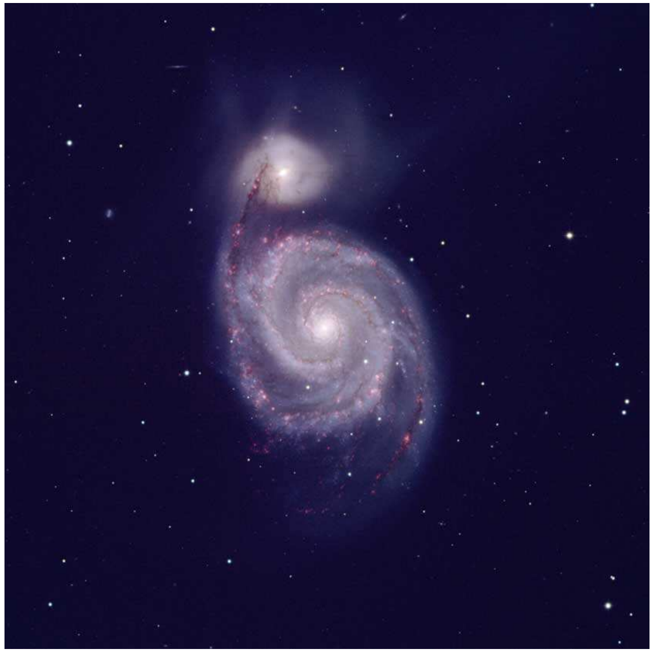

M51, NOAO, T. Rector

NGC 4565, McLaughlin

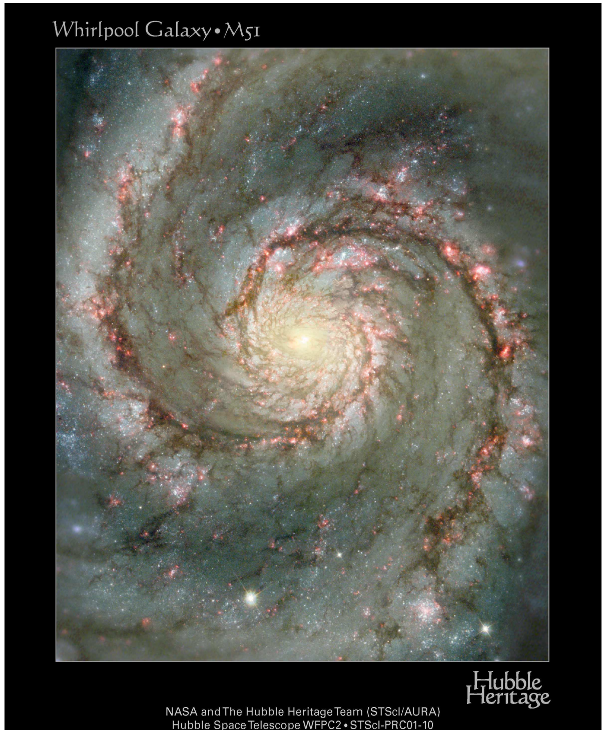

Whirlpool Galaxy • M51

Hubble Heritage

NASA and The Hubble Heritage Team (STScI/AURA)
Hubble Space Telescope WFPC2 • STScI-PRC01-10

Star Forming Region RCW 108 in ARA
(MPG/ESO 2.2-m + WFI)

ESO PR Photo 21a/99 (30 April 1999)

© European Southern Observatory

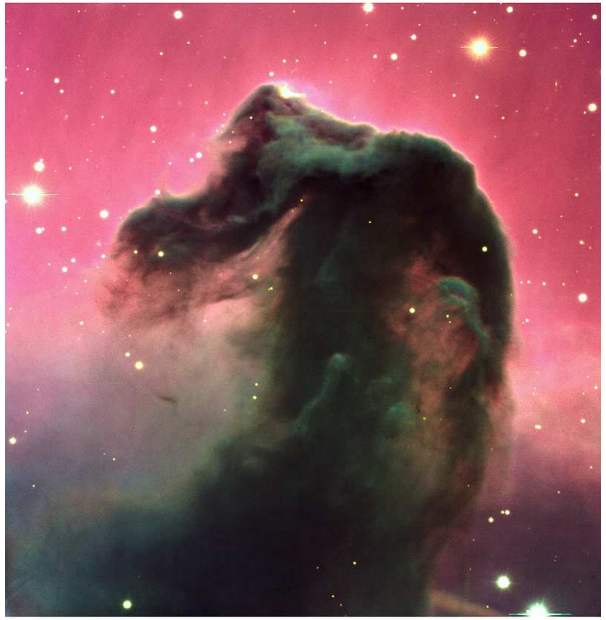

The Horsehead Nebula
(VLT KUEYEN + FORS 2)

ESO PR Photo 02a/02 (25 January 2002)

© European Southern Observatory

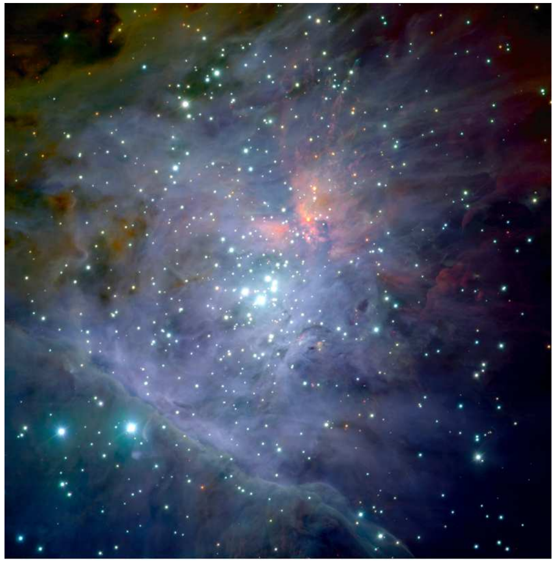

The Orion Nebula and Trapezium Cluster
(VLT ANTU + ISAAC)

ESO PR Photo 03a/01 (15 January 2001)

© European Southern Observatory

Reflection Nebula NGC 1999

PRC00-10 • Space Telescope Science Institute • NASA and The Hubble Heritage Team (STScI)

Milky Way: ISM

The ISM of the Milky Way consists of the following phases

Name	Type	n cm^{-3}	T K	Filling Factor Vol-%	Mass % ISM	Comments
HIM	H II	10^{-2}–10^{-4}	10^{6}–10^{8}	20–60	<1	SNR, wind, shocks
WIM	H II	10^{-1}–10^{-4}	10^{4}	1–10	<1	photoionized by O/B-stars
WNM	H I	1–10	10^{4}	20–30	20-50	21cm clouds, shells
CNM	H I	10–10^{2}	100	10–20	20-50	HI envelopes, shells
MC	H I	10^{2}–10^{4}	10	1	40-50	IR, dust

HIM: Hot Ionized Medium, WIM: Warm Ionized Medium, WNM: Warm Neutral Medium, CNM: Cool Neutral Medium, MC: Molecular Clouds

courtesy J. Bally

Molecules: History

- Secchi, 1878: First notice of molecular features in stellar spectra (class III and IV; no explanation)
  Today known as TiO, C_2, and CN bands
- 1930s: Molecular lines in spectra of planetary atmospheres and comets as well as low temperature stars
- 1941: Interstellar absorption lines due to CN, CH, and CH^+ in optical spectrum of ζ Oph
- Weinreb et al, 1963: Radio absorption lines at $\lambda = 18\,\mathrm{cm}$ from OH towards SNR Cas A (not associated with Cas A, but with foreground clouds). masers (=non-LTE!)
- Cheung et al., 1968: First multi-atom molecules: NH_3 and H_2O ($\lambda = 1.35\,\mathrm{cm}$).
- Snyder et al., 1969: Formaldehyde (H_2CO).
- Today: more than 120 different molecules known

Molecular Hydrogen

Because of high abundances: most molecular gas is H_2.

For review of properties of H_2, see Shull & Beckwith, 1982, Ann. Rev. Astron. Astrophys. 20, 163

H_2 is homonuclear

$\Longrightarrow$ no permanent dipole moment

$\Longrightarrow$ no rotational dipole transitions.

Only transitions observable are vibrational or electronic.

Vibrational: $\lambda \sim 6\,\mu\mathrm{m}$, in the infrared.

Problem: Dust extinction in IR severe

Once H is molecular, it is very difficult to see.

Alternative: Observation of electronic transitions of H_2 in absorption against hot UV-Stars (“Werner-bands”).

Note that excitation of transitions requires lots of energy which cannot be produced otherwise.

Molecular Hydrogen

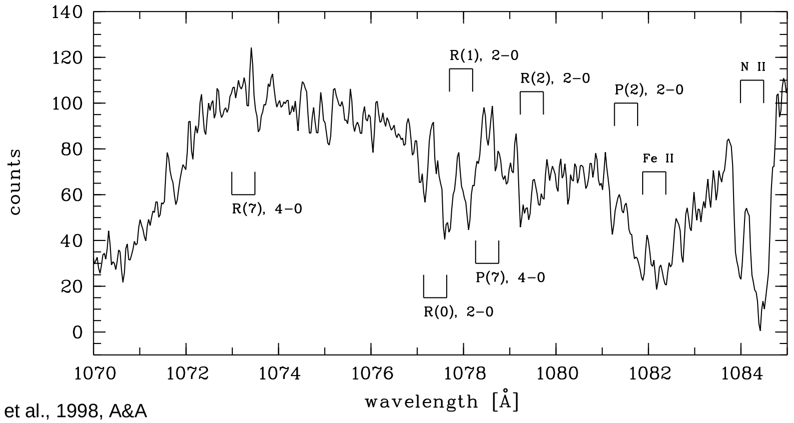

Richter et al., 1998, A&A

ORFEUS: Discovery of H_2 bands in absorption in direction towards SMC

$\Longrightarrow$ H_2 also present in diffuse ISM, not only in clouds

(agrees with *Copernicus* measurements in milky way; Spitzer, 1974)

Molecular Hydrogen

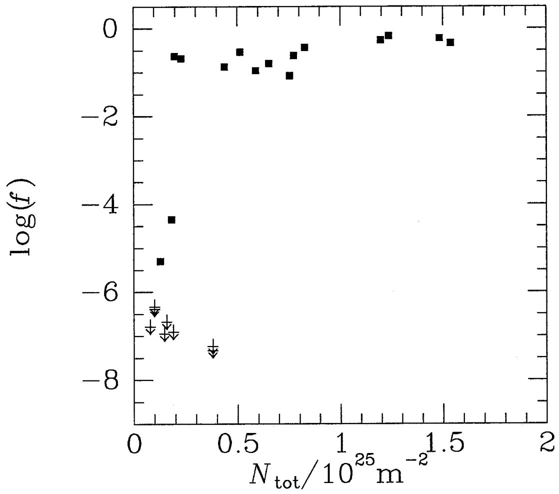

Binney&Merrifield, Fig. 8.5

Calculate total Hydrogen-density obtained from

$$N(\mathrm{H_{tot}}) = N(\mathrm{HI}) + 2N(\mathrm{H_2}) \quad (3.6)$$

and molecular fraction

$$f_{\mathrm{H_2}} = \frac{2N(\mathrm{H_2})}{N(\mathrm{H_{tot}})} \quad (3.7)$$

For $N(\mathrm{H_{tot}}) < 2 \times 10^{18}\,\mathrm{cm}^{-2}$, i.e., low columns, H is atomic, above that molecular $\Longrightarrow$ More molecules in denser parts of ISM.

Carbon Monoxide

Better than observing H_2 directly is to deduce its presence *indirectly* using other molecules with rotational positions $\Longrightarrow$ use heteronuclear molecules, e.g., CO, CS, HCN.

Candidate Number 1: CO, rotational transitions at 1.3 mm ($J = 2 \rightarrow J = 1$) and 2.6 mm ($J = 1 \rightarrow J = 0$).

Notation: CO(2-1) and CO(1-0)

CO is less abundant than H_2 (see later), but Einstein A-coefficients of lines very large; $\tau = 1$ reached at CO-column $\sim 6 \times 10^{15}\,\mathrm{cm}^{-2}$, corresponding to $N_\mathrm{H} \sim 8 \times 10^{19}\,\mathrm{cm}^{-2}$

$\Longrightarrow$ Cannot use “standard” CO to look into thick clouds.

$\Longrightarrow$ Use some tricks: Isotope effects!

CO: Isotope Effects

CO occurs in several forms:

- $^{12}C^{16}O$ (= ^{12}CO)
- $^{13}C^{16}O$ (= ^{13}CO)
- $^{12}C^{18}O$ (= $C^{18}O$)

because of slightly different reduced masses, wavelength of transitions slightly different $\Longrightarrow$ can separate emission lines from these species.

Relative abundances:

$^{12}CO : {}^{13}CO : C^{18}O = 500 : 65 : 1$

By using ^{13}CO or $C^{18}O$, can look deeper in molecular cloud.

Column from Lines

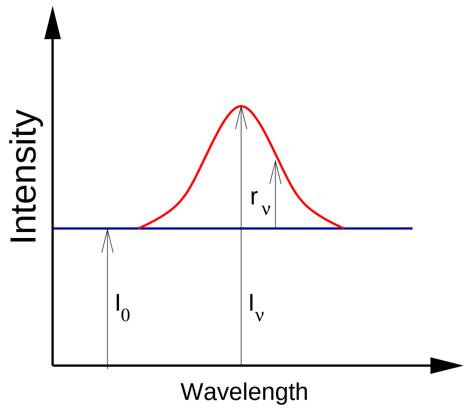

after Cowley, Fig. 14.5

To measure mass from emission line, determine number of emitting atoms, N.

Observed intensity not trivially $\propto N$ because of self-absorption.

Excess in line:

$$r_\nu = \frac{I_\nu - I_0}{I_0} = \frac{S_\nu - I_0}{S_\nu}\left(1 - \exp\left(-\frac{\tau_\nu}{\mu}\right)\right) \quad (3.8)$$

where τ: optical depth, I_0: background intens., $\mu = \cos\theta$

Inserting τ in terms of transition probability f_{nm} and expanding the exponential gives for the equivalent width

$$W_\nu = \int r_\nu \,\mathrm{d}\nu \sim \frac{\pi e^2}{mc} r_0 f_{nm} \frac{N_n}{\mu} \quad (3.9)$$

where $r_0 = (S_\nu - I_0)/S_\nu$.

courtesy Matthew T. Russell

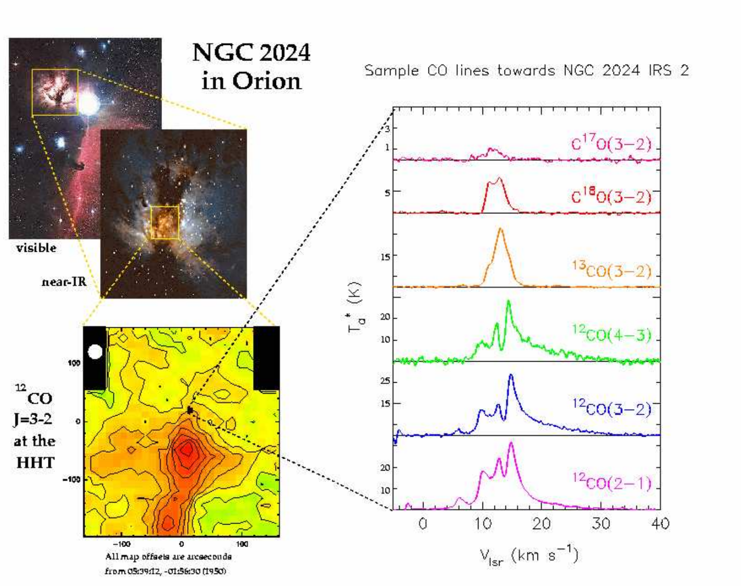

(courtesy Craig Kulesa)

As a case study: use NGC 2024 (flame nebula, bright star is Alnitak [ζ Ori]).

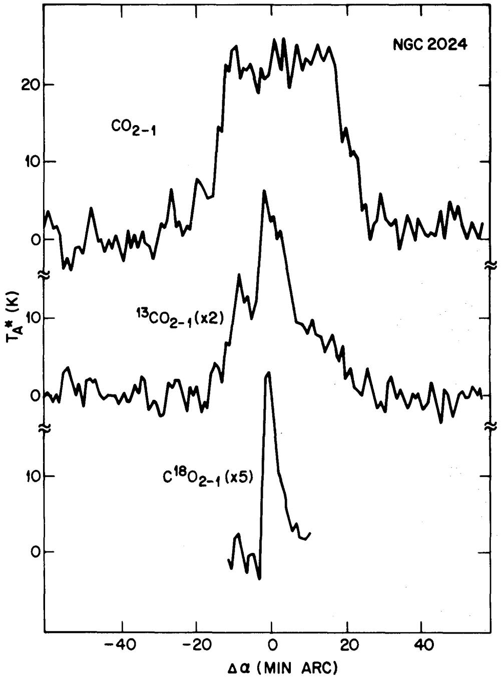

Right-ascension strip maps over NGC 2024: peak intensities ^{12}CO, ^{13}CO, and C^{18}O scale as 5:2:1 $\Longrightarrow$ cloud is optically thick (lines should scale as the abundances, and they don't).

Last step to obtain N_{CO}: use Boltzmann if (and only if) LTE is appropriate…

(Phillips et al., 1979, Fig. 3b), Intensity given as antenna temperature, $I = 2kT\nu^2/c^2$.

From CO to H

Once $N(\text{CO})$ has been determined: Infer H$_2$ column using some “standard” ratio. Typical assumptions:

$$\frac{N(^{13}\text{CO})}{N(\text{H}_2)} \sim 0.5\ldots2.0\times10^{-6} \tag{3.10}$$

Ratio determined from UV-data on hydrogen and CO measurements at cloud edges (low τ).

Caveats:

- CO usually *not* in LTE for higher J
- $n(\text{H}_2)/n(^{12}\text{C})$, $n(^{12}\text{C})/n(^{13}\text{C})$ affected by astration (passage of ISM through stars), $\Longrightarrow$ $n(^{12}\text{C})/n(^{13}\text{C}) = 20$ at GC, 90 at large Galactic radii,
- Clumpy clouds? Shadowing? (finite beamsize of telescope…),
- Isotope ratios very different between different cloud complexes
- …

H$_2$ mass only determinable to factor of a few!

Molecular Clouds

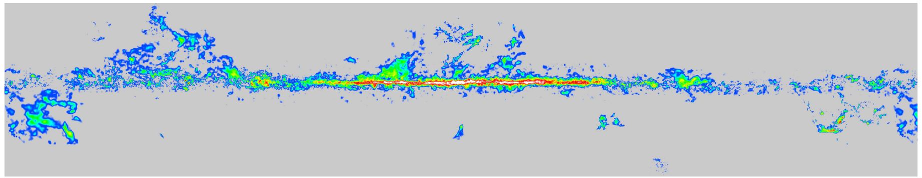

Dame et al., CfA; Columbia 1.2 m telescope

CO distribution in galactic coordinates: concentration of clouds on plane; high speed at center not yet understood.

Molecular Clouds

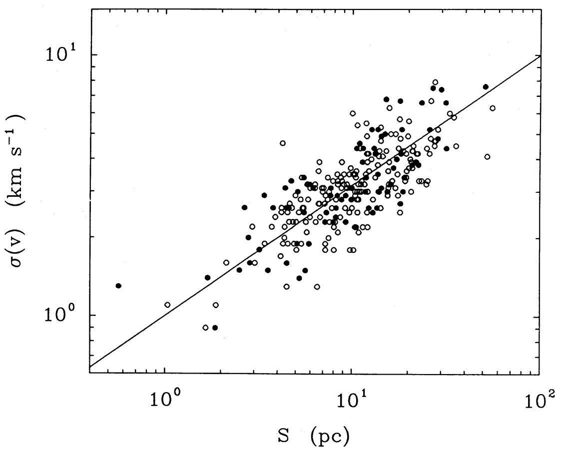

Solomon et al. (1987): 2.6 mm ^{12}CO survey of $>$ 200 molecular clouds within solar circle.

Relationship between velocity dispersion, σ_v, (from line width) and cloud size, S:

$$\sigma_v = (1 \pm 0.1)\,\mathrm{km\,s^{-1}} \left(\frac{S}{\mathrm{pc}}\right) \tag{3.11}$$

(Solomon et al., 1987, Fig. 1)

Molecular Clouds

Median linewidth in Solomon survey:

$$\sigma_v \sim 3\,\mathrm{km\,s^{-1}} \tag{3.12}$$

Compare to sound-speed, assuming $kT \sim 30\,\mathrm{K}$

$$c_\mathrm{s} \sim \sqrt{\frac{kT}{m_\mathrm{p}}} \sim 0.5\,\mathrm{km\,s^{-1}} \sqrt{\frac{T}{30\,\mathrm{K}}} \tag{3.13}$$

σ_v dominated by turbulent velocity within clouds, not by sound speed. . .

Turbulent pressure $P \sim nm\sigma_v^2$, with $n \gtrsim 10^2\,\mathrm{cm^{-3}}$, much higher than confining pressure in intra-cloud medium (there: $n \sim 1\,\mathrm{cm^{-3}}$, $c_s \sim 10\,\mathrm{km\,s^{-1}}$) $\Longrightarrow$ clouds confined by gravity!

Use virial theorem to obtain mass:

$$M \sim \mathrm{const.}\frac{\sigma_v^2 S}{G} \tag{3.14}$$

where const. ~ 8.7, depending on geometry.

Molecular Clouds

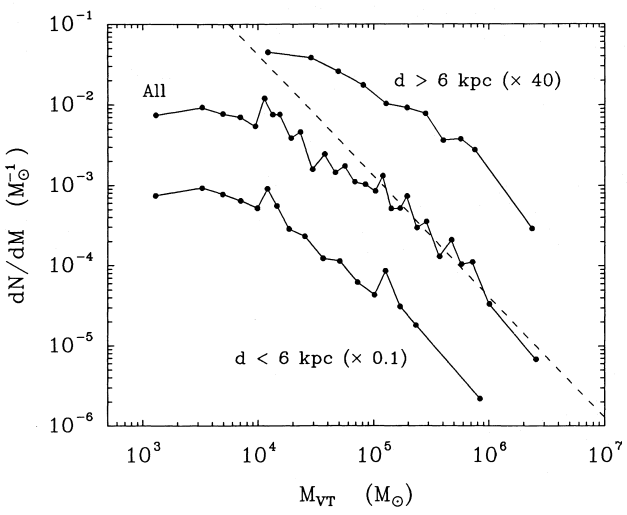

Mass spectrum of molecular clouds is roughly

$$\frac{\mathrm{d}N}{\mathrm{d}M} \propto M^{-1.7} \tag{3.15}$$

for $2000\,\mathrm{M_\odot} < M < 40000\,\mathrm{M_\odot}$.

At low masses selection effect (biasing).

Integrating over mass distribution shows

Most of the Galaxy's molecular gas is in the most massive clouds

(Solomon & Rivolo, 1989, Fig. 1)

Molecule Formation

Formation of molecules in dense media (e.g., Earth's atmosphere) is no problem. This is very different from the rest of the universe!

Assume two-body collision of two (neutral) atoms: typical interaction timescale $10^{-13}\,\mathrm{s}$ (1 vibration timescale).

To form molecule, need to get rid of excess energy!

Problem: Typical time for radiative relaxation given by A-coefficient ($\sim 10^8\,\mathrm{s^{-1}}$)

$\Longrightarrow$ Typical collisional time-scale too low

$\Longrightarrow$ cannot form molecules!

On Earth, excess energy carried away by triple-collisions, these are too rare in the ISM. . .

Further complication: UV-dissociation of molecules.

Molecule Formation

Solution: “nonstandard chemistry”, i.e., Atom-ion reactions and dust as catalyst

Atom-ion reactions are, e.g.,

$$O^+ + H_2 \longrightarrow OH^+ + H \tag{3.16}$$

These reactions are very effective since the ion polarizes the molecule.

Langevin theory:

Assume charge q_1 approaches molecule; represent induced dipole-moment by charge q_2 separated by distance p. Then

$$q_2 p = \alpha E \tag{3.17}$$

where E electric field, α polarizability. Since $E = q_1/r^2$, this means

$$p = \frac{\alpha q_1}{q_2 r^2} \tag{3.18}$$

and the attractive force is

$$F_r = -\frac{2q_1q_2p}{r^3} = -\frac{2q_1^2\alpha}{r^5} \tag{3.19}$$

Molecule Formation

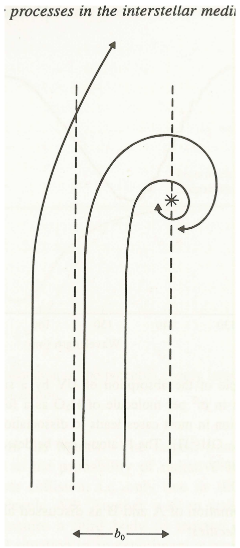

Thus the potential energy is

$$V(r) = \int_r^\infty F_r \,\mathrm{d}r = \frac{q_1^2\alpha}{2r^4} \tag{3.20}$$

Motion in such a potential allows spiral-in (F can not always be balanced by centrifugal force).

This happens for impact parameters $b < b_0$ where

$$b_0 = q_1 \left(\frac{4\alpha}{\mu v^2}\right)^{1/4} \tag{3.21}$$

where μ is the reduced mass.

$\Longrightarrow$ Langevin cross section

$$Q = \pi b_0^2 \propto \frac{1}{v_\infty} \tag{3.22}$$

Since the collision frequency $\propto \langle Qv \rangle$, collision frequency is independent of energy

Not really true in full theory, but dependence small for regime of astrophysical interest.

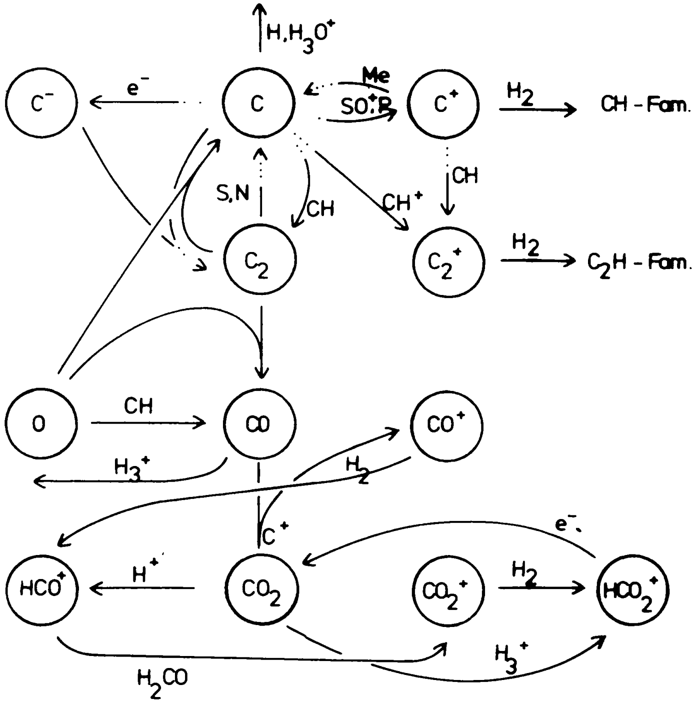

Typical theory of molecular formation: reaction networks with ∼1000 and more different reactions.

Henning, 1981

Hydrogen Molecule

One unavoidable fact: we cannot produce H_2 in gas phase $\Longrightarrow$ this must occur on surface of dust grains.

Why?

Two-body recombination is not possible because H_2 has no dipole moment $\Longrightarrow$ radiative relaxation would go via quadrupole terms, which is very slow.

Therefore: the general picture is:

adsorption of H on grain surface (e.g., ice, silicate) $\Longrightarrow$ proton will thermally “hop” over surface (tunnel through lattice structure,. . .) $\Longrightarrow$ Two H-atoms meet $\Longrightarrow$ formation of H_2

Detailed theory requires knowledge about grains.

Dust

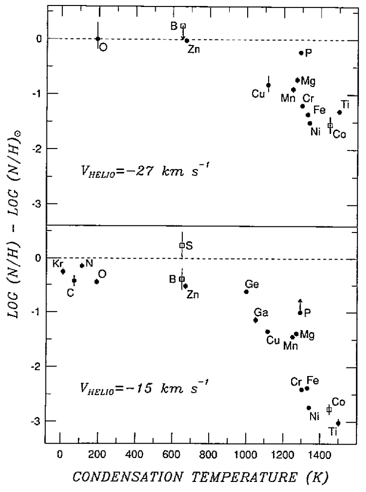

Evidence for existence of solid state material in universe comes mainly from two observations:

1. Depletion of elements in ISM gas phase wrt. solar abundances
2. Reddening of stars

Abundances in direction to ζ Oph (Federman et al., 1993)

Extinction

Extinction = dimming of starlight by dust

How is this measured?

Assume two stars, 1,2, at distances d_1, d_2, with same physical spectral shape, $F(\lambda)$. Medium to star 2 has optical depth $\tau(\lambda)$. Observed spectral fluxes are

$$F_1(\lambda) = \frac{F(\lambda)}{d_1^2} \quad \text{and} \quad F_2(\lambda) = \frac{F(\lambda)}{d_2^2}\mathrm{e}^{-\tau(\lambda)} \tag{3.23}$$

Compare fluxes at wavelength λ_1:

$$\frac{F_1(\lambda_1)}{F_2(\lambda_1)} = \frac{F(\lambda_1)/d_1^2}{F(\lambda_2)/d_2^2}\mathrm{e}^{\tau(\lambda_1)} = \frac{d_2^2}{d_1^2}\mathrm{e}^{\tau(\lambda_1)} \tag{3.24}$$

Same at λ_2:

$$\frac{F_1(\lambda_2)}{F_2(\lambda_2)} = \frac{d_2^2}{d_1^2}\mathrm{e}^{\tau(\lambda_2)} \tag{3.25}$$

Therefore

$$\frac{F_1(\lambda_1)/F_1(\lambda_2)}{F_2(\lambda_1)/F_2(\lambda_2)} = \mathrm{e}^{\tau(\lambda_1)-\tau(\lambda_2)} \tag{3.26}$$

Extinction

Take the logarithm of both sides and multiply with -2.5:

$$-2.5\log\left(\frac{F_1(\lambda_1)}{F_1(\lambda_2)}\right) - \left(-2.5\log\left(\frac{F_2(\lambda_1)}{F_2(\lambda_2)}\right)\right) = \text{const.}\cdot(\tau(\lambda_1)-\tau(\lambda_2)) \tag{3.27}$$

Now remember the definition of the magnitude

$$m(\lambda_1) - m(\lambda_2) = -2.5\log\frac{F(\lambda_1)}{F(\lambda_2)} \tag{3.28}$$

Therefore Eq. (3.27) reads

$$(m_1(\lambda_1) - m_1(\lambda_2)) - (m_2(\lambda_1) - m_2(\lambda_2)) = \text{const.}\cdot(\tau_1 - \tau_2) \tag{3.29}$$

In astronomy, a color is defined as a difference of magnitudes, e.g. for the B- and V-filters:

$$\mathrm{B}-\mathrm{V} = m(\mathrm{B}) - m(\mathrm{V}) \tag{3.30}$$

Thus, Eq. (3.29) is difference between colors, or color excess

$$E_{\lambda_1-\lambda_2} := (m_1(\lambda_1) - m_1(\lambda_2)) - (m_2(\lambda_1) - m_2(\lambda_2)) \tag{3.31}$$

Note that because of Eq. (3.29)

$$E_{\lambda_1-\lambda_2} \propto \tau_1 - \tau_2 \tag{3.32}$$

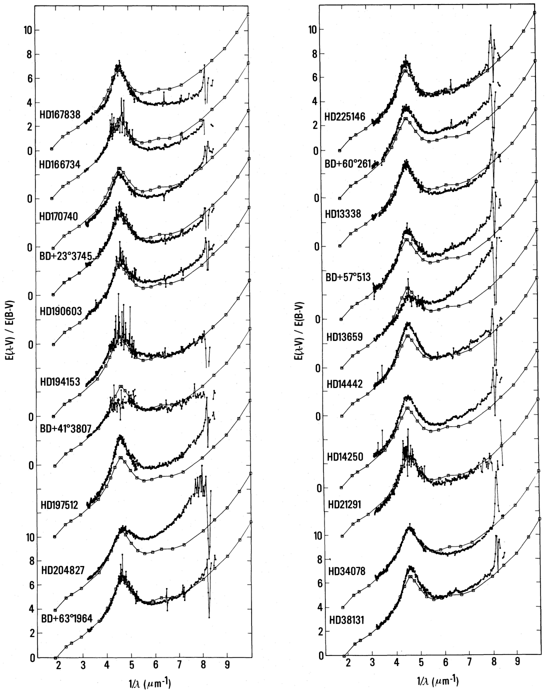

Generally, we use normalized color excess,

$$\frac{E(\lambda-\mathrm{V})}{E(\mathrm{B}-\mathrm{V})} = \frac{\tau(\lambda)-\tau(\mathrm{V})}{\tau\mathrm{B}-\tau\mathrm{V}} \tag{3.33}$$

$$\propto \frac{\tau(\lambda)-\tau(\mathrm{V})}{\tau(\mathrm{B})-\tau(\mathrm{V})} \tag{3.34}$$

$$\propto \tau(\lambda) \tag{3.35}$$

$$\propto \sigma_{\mathrm{sca}}(\lambda) \tag{3.36}$$

Stellar spectra in the UV (Witt et al., 1984): Overall the extinction is very similar, there is a prominent feature at $1/\lambda \sim 4.6$ ($\lambda = 2170$ Å), the strength of the feature varies, but its position is very stable.

Extinction

Observationally important is relationship between reddening $E(\mathrm{B}-\mathrm{V})$ and extinction in V-band.

Extinction defined via

$$A_\mathrm{V} = \mathrm{V} - \mathrm{V}_0 \tag{3.37}$$

Now, normalized extinction was

$$\frac{E(\lambda-\mathrm{V})}{E(\mathrm{B}-\mathrm{V})} = \frac{(m_\lambda - m_\mathrm{V}) - (m_\lambda - m_\mathrm{V})_0}{E(\mathrm{B}-\mathrm{V})} \tag{3.38}$$

$$= \frac{m_\lambda - m_{\lambda,0} - (m_\mathrm{V} - m_{\mathrm{V},0})}{E(\mathrm{B}-\mathrm{V})} \tag{3.39}$$

$$= \frac{A_\lambda - A_\mathrm{V}}{E(\mathrm{B}-\mathrm{V})} \tag{3.40}$$

But for $\lambda \to \infty$:

$$\frac{E(\lambda-\mathrm{V})}{E(\mathrm{B}-\mathrm{V})} \longrightarrow \text{const.} =: R \tag{3.41}$$

where $R \sim 3.1 \pm 0.1$.

$\Longrightarrow A_\mathrm{V}$ known if $E(\mathrm{B}-\mathrm{V})$ known!

Note also that $A_\mathrm{V}/E(\mathrm{B}-\mathrm{V}) \propto r$ since $\tau = n\sigma_\mathrm{scat} r$

$\Longrightarrow$ can measure distance! Generally, $A_\mathrm{V} \sim 1\ldots2\,\mathrm{mag\,pc}^{-1}$.

Extinction

The normalized reddening observed is roughly $\propto 1/\lambda$.

Explanation: scattering of radiation on grains.

The overall theory is very complicated, so only show the rough idea here…

In scattering, intensity is

$$I = I_0 \exp(-n\pi a^2 Q l) \tag{3.42}$$

where the quality factor Q has two components:

$$Q = Q_\mathrm{abs} + Q_\mathrm{sca} \tag{3.43}$$

Q_abs: absorption,

Q_sca: scattering.

(see next slide)

Note that Q is proportional to the optical depth…

Define the Albedo of particles

$$\gamma = \frac{Q_\mathrm{sca}}{Q_\mathrm{abs} + Q_\mathrm{sca}} \tag{3.44}$$

(note that in principle there is also an angular dependence)

Extinction

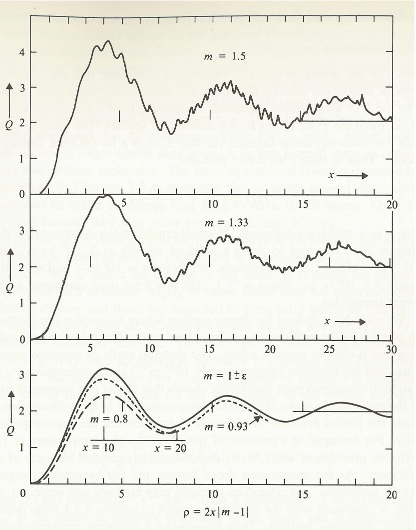

4.5. Extinction curves for spheres computed from Mie's formula for m =

Detailed theory: Mie scattering; gives $Q \propto 1/\lambda$ for small diameters $a \Longrightarrow$ as observed!

Q_sca as a function of $x = 2\pi a/\lambda$ for several dielectric constants m (Dyson& Williams, Fig. 4.5; $m = 1.33$ is water ice)

Extinction

For detailed theory also need size distribution of grains.

Common assumption:

$$n(a) = Aa^{-3.5} \tag{3.45}$$

("MRN distribution"; Mathis, Rumpl, Nordsieck; $0.005\,\mu\mathrm{m} < a < 0.25\,\mu\mathrm{m}$) determined from fitting extinction curves.

Overall $1/\lambda$-behavior is understood as being due to Mie scattering

2200 Å feature:

- graphite grains? Optical constants change dramatically around 2200 Å for small graphite grains.
- Silicate grains?
- Polycyclic aromatic hydrocarbons (PAHs)?

Dust Models

Major dust models:

- MRN model
- Core-mantle models
- post-IRAS models

Models must take constraints on dust models into account:

- extinction curve (IR to UV)
- abundance deficiency of ISM gas phase
- (narrow) spectral features

See Witt, IAU Symp. 197, for a discussion of results.

UIBs

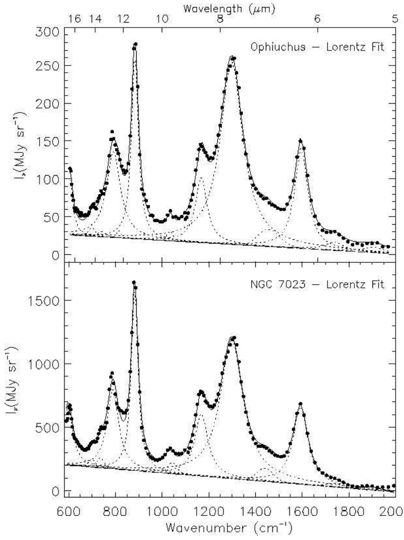

Unidentified emission structures seen at 3.3, 6.2, 7.7, 8.6, 11.3 μm seen in H II regions, YSOs, diffuse ISM, and even AGN: "unidentified infrared bands"

(Boulanger et al.; 1998)

PAHs

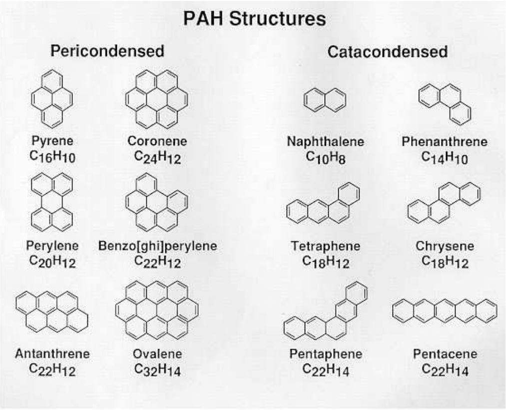

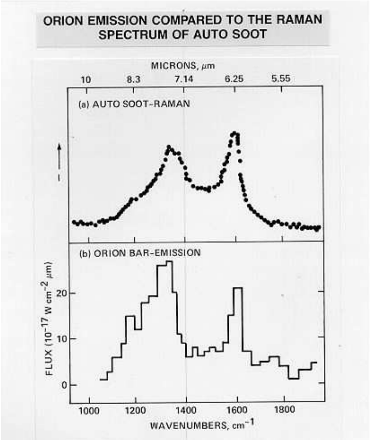

UIB emission is probably due to polycyclic aromatic hydrocarbons (PAHs), complex large carbonaceous molecules (UIB: related to C-C, C-H modes)

PAHs

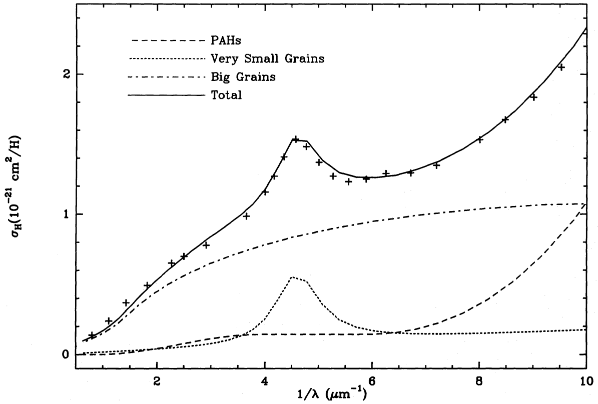

Inclusion of PAHs in dust models can also account for extinction curve, need three distinct populations:

- big grains (15 nm to 110 nm),
- very small grains (1.2 nm to 15 nm)
- PAHs (<1.2 nm)

Also predicts UIB emission!

Dśert, Boulanger, Puget (1990)

A problem with the Désert et al. model is the small size of large grains, which is inconsistent with X-ray halos. . . Possible solution: fluffy grains (Fogel & Leung, 1998)

Dust Formation

Where does dust come from?

Three potential sources:

1. Condensation out of the ISM
2. Condensation in cool stellar outflows
3. Condensation in protostars

ad 1) only possible in very dense molecular clouds: formation of clusters of 10. . . 20 atoms as “condensation nuclei”; accretion of further molecules via collisions.

Due to small densities dust formation timescale very long (10^8 years), thus rather impossible.

Dust is mainly generated in stars and then ejected into the ISM.

Dust Formation

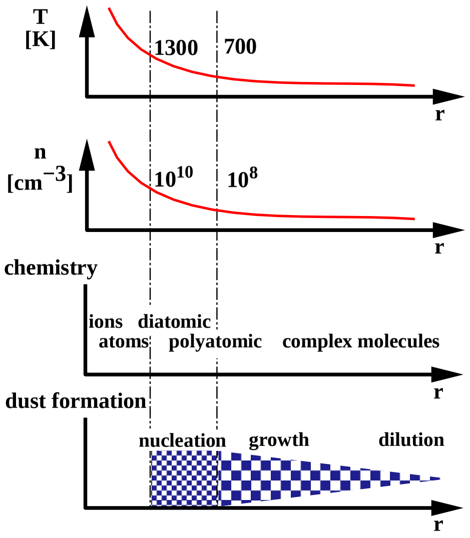

Dust formation in stars

Stellar atmospheres have much higher density than GMCs (solar photosphere: 10^{17} cm^{-3}, late type giants: $\sim$ 10^{15} cm^{-3}, compared to 10^6 cm^{-3} in GMCs)

$\Longrightarrow$ much higher condensation probability.

General process:

1. formation of molecules
2. accretion of more material, formation of clusters
3. formation of macroscopic particles

(Sedlmayr & Krüger; 1997)

Dust Formation

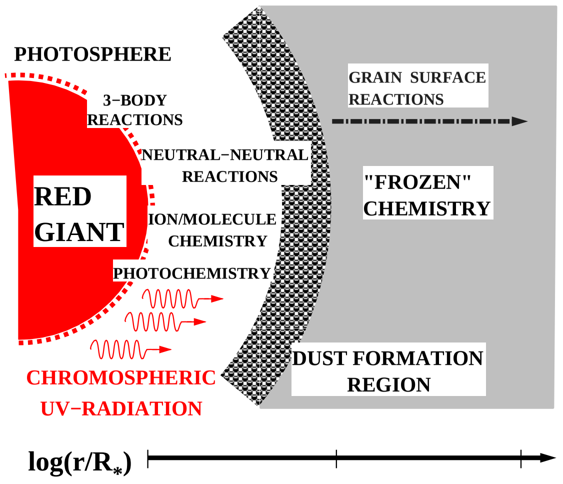

(Sedlmayr & Krüger; 1997)

Complex nonstationary chemistry makes things very complicated. . .

Dust Formation

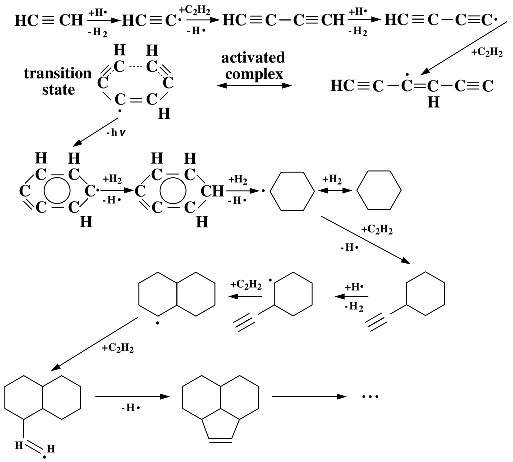

(Sedlmayr & Krüger; 1997)

Possible chemical reaction network for generation of PAHs in C-stars.

Bekki K., Chiba M., 2009, Proc. Astron. Soc. Aust. 26, 48

Gordon K.D., Bailin J., Engelbracht C.W., et al., 2006, ApJ 638, L87

Kim S., Staveley-Smith L., Dopita M.A., et al., 1998, ApJ 503, 674

Mateo M.L., 1998, ARA&A 36, 435

Mathewson D.S., Cleary M.N., Murray J.D., 1974, ApJ 190, 291

Meixner M., Gordon K.D., Indebetouw R., et al., 2006, AJ 132, 2268

Putman M.E., Staveley-Smith L., Freeman K.C., et al., 2003, ApJ 586, 170

Solomon P.M., Rivolo A.R., 1989, ApJ 339, 919

Solomon P.M., Rivolo A.R., Barrett J., Yahil A., 1987, ApJ 319, 730